Bull. Mater. Sci., Vol. 40, No. 3, June 2017, pp. 527–535
DOI 10.1007/s12034-017-1402-4

Polymer-assisted co-precipitation route for the synthesis of Al_2O_3–13% TiO_2 nanocomposite

NEERA SINGH[1,2,*], RANABRATA MAZUMDER[1], PALLAV GUPTA[3] and DEVENDRA KUMAR[2]
[1]Department of Ceramic Engineering, National Institute of Technology-Rourkela, Rourkela 769008, India
[2]Department of Ceramic Engineering, Indian Institute of Technology (B.H.U.), Varanasi 221005, India
[3]Department of Mechanical and Automation Engineering, A.S.E.T., Amity University, Uttar Pradesh, Noida 201313, India
*Author for correspondence (neera.rs.cer14@itbhu.ac.in)

MS received 26 April 2016; accepted 9 August 2016; published online 9 June 2017

Abstract. The present investigation reveals the effect of processing parameters on the properties of alumina–titania (Al_2O_3–TiO_2) nanocomposites. A polymer-assisted (Pluronic P123 triblock co-polymer) co-precipitation route has been employed to synthesize Al_2O_3–TiO_2 nanoparticles. As a surfactant, pluronic P123 polymer exhibits hydrophobic as well as the hydrophilic nature simultaneously which detains the agglomeration and hence the nano size particle have been obtained. Effect of surfactant concentration on morphology and particle size of product has also been investigated. Thermal behaviour of the prepared powder samples have been studied using differential scanning calorimeter/thermal gravimetric analysis and dilatometer. Formation of aluminium-titanate (Al_2TiO_5) phase has been confirmed using X-ray diffraction analysis. It has been observed by field emission scanning electron microscopy analysis that the particle size reduced effectively (below 100 nm) when polymer-assisted co-precipitation route is used instead of the simple co-precipitation technique. A highly dense microstructure of sintered samples has been obtained, driven by reduced particle size.

Keywords. Co-precipitation; DSC/TGA; XRD; FESEM; dilatometry.

1. Introduction

An overall fast growing modernization demands a spark in the development of advanced ceramics, which are essential for severe structural applications. Naturally occurring or conventionally used materials such as metals and clay-based ceramics seem to deny the promises that are required for higher temperature and such adverse conditions. In the past few decades, there has been a breakthrough and ceramic matrix composites are proposed to be a promising candidate for such applications. Ceramic matrix composites are basically a class of materials in which both the matrix and reinforcement phases are composed of ceramics. In general, they are used in various structural applications such as rockets, jet engines, gas turbines, heat shields for space vehicles, fusion reactors and heat treatment furnaces [1]. Reinforcement phases provide strength, whereas the matrix itself supports the whole structure, which results in a product with superior mechanical and thermal properties; a scope to be used in severe working environment. Among all the ceramic matrix composites, alumina–titania (Al_2O_3–TiO_2) composites are preferable for high performance coating applications where large thermal barriers are used. Al_2O_3–TiO_2 composites are well known for their high toughness, low thermal expansion, low thermal conductivity, high adhesion strength and most importantly high thermal shock resistance. Above all, they also exhibit excellent abrasive wear resistance to high temperature erosion as well as better cryogenic compatibility. Metals when compared with Al_2O_3–TiO_2 composites, show low emissivity over the whole radiation spectrum and thus cannot dissipate heat by radiating in the thermal infrared region. It is well known that most ceramic materials show strong efficiency of photon emission thus exhibiting a high emissivity value. Al_2O_3–TiO_2 coating have high thermal emissivity (>0.95) [2]. The sintered form of Al_2O_3–TiO_2 composite shows the aluminium-titanate (Al_2TiO_5) phase, which exists in two allotropic forms, i.e., α and β, where β is the low temperature phase [3]. It is evident from literature that the presence of Al_2TiO_5 phase improves the thermo-mechanical property of the composite. Therefore, Al_2O_3–13 wt% titania (TiO_2) composite is studied by most of them, owing to its better thermo-mechanical property. Commercially available Al_2O_3–13 wt% TiO_2 composite powder having particle size in the range of few microns is named as Metco 130. It has been found that coatings of Al_2O_3–13 wt% TiO_2 nanoparticles have better properties like high abrasive wear resistance, better fracture toughness and good bond strength than the properties of Metco 130 [4,5]. To get final fine-grained and dense microstructure composite, it is required to produce precursor nano-powder. Final properties are derived by each phase present in the material and hence it would be essential if effects are tailored up to the

raw level. Initial parameters such as composition, preparation route, particle size and sintering temperature are prime factors of concern to achieve desired phase and properties in the material. However, while focusing on such properties, primarily, the density of material should be considered. Interestingly, the density can be altered just with a slight change in the processing conditions. Therefore, the preparation route must be selected carefully considering the desired density as well as other physical, mechanical, structural properties etc., respectively. Solid state, plasma spraying, sol–gel method and laser smelting are such popular routes to synthesize Al_2O_3–13 wt% TiO_2 composite. Okamura *et al* [6] prepared a non-agglomerated, mono-sized Al_2O_3–TiO_2 composite powder by the stepwise hydrolysis of titanium alkoxide in Al_2O_3 dispersion. Particle size was controlled by selecting the size of starting Al_2O_3 powder, whereas amount of TiO_2 was determined by the amount of hydrolysed alkoxide. Al_2O_3–TiO_2 composite-powder compact containing 50 mol.% TiO_2, when fired at 1350°C for 30 min showed theoretical density close to Al_2TiO_5 (3.70 g cm^{-3}) phase. Jayasankar *et al* [7] prepared nano size alumina—Al_2TiO_5 composite through a titania-coated alumina particle precursor. They have used $TiCl_4$ as precursor of TiO_2 that is hazardous and costly. The starting alumina particle size has no significant influence on the formation temperature of Al_2TiO_5 in the composite. X-ray diffraction (XRD) analysis confirms the formation of Al_2TiO_5 after sintering at 1350°C and with 98% sintered density.

Few ressearchers have worked on polymer-assisted chemical routes to achieve the final material in nano size range. Among these, the polymer-assisted co-precipitation route has gained attention of many researchers for achieving the demand of synthesizing nano size powders and highly dense microstructures. Processing of this route is simple and stearic state of the particle surface along with overall homogeneity is maintained. Amount of polymer, solubility of different reactants, precipitation rate, as well as drying and firing schedule can affect the particle size, morphology and phase formation. Few of the researchers have worked on polymer-assisted synthesis routes for selected systems to achieve desired properties. Example, Landeros *et al* [8] synthesized the Li_2SiO_3 powders by hydrothermal crystallization using TRITON X-114 as the surfactant. Microstructure of synthesized powder revealed hollow microspheres with high surface area of about 69.5 $m^2\,g^{-1}$. Huang *et al* [9] reported the synthesis of hydroxyapatite (HA) by co-precipitation route using tri-block co-polymer F127 as a surfactant. Use of a surfactant helped in getting uniform nanoparticles as compared to the HA prepared without using any surfactant. Synthesized HA was found to have controlled structural properties with their usefulness in biomedical applications. Mosayebi *et al* [10] reported the effect of surfactant used in co-precipitation route as well as the effect of other parameters such as refluxing temperature, time and calcination temperature on the synthesis of magnesium aluminates ($MgAl_2O_4$) spinel. Successful synthesis of nano crystalline ($MgAl_2O_4$) with high surface area was achieved due to the addition of pluronic P123 triblock co-polymer.

There are few reports on *in-situ* synthesis of Al_2O_3–TiO_2 composite powder by wet chemical method [11–13]. Study of the effect of polymer concentration on morphology as well as sintering behaviour of Al_2O_3–TiO_2 composite material has not been investigated to a large extent. Therefore, the present investigation has been focused on the preparation of Al_2O_3–TiO_2 composite by using polymer-assisted co-precipitation technique, leading towards complete conversion of TiO_2 into Al_2TiO_5 phase in a sintered product. Synthesized powder was found in nano size range. Investigations were also done on the morphology and sintering behaviour of the prepared material. Achieved density was found to be better than other conventional methods. Density of the sintered material has increased with increasing polymer content during synthesis. However, a reverse effect (i.e., agglomeration between grains) was seen in the synthesized powder, which resulted in decrease in the density of sintered samples when polymer concentration is 100%. Total amount of Al_2TiO_5 phase also increased with increasing polymer content in the initial solution. This enhancement in Al_2TiO_5 phase is due to the high reactivity of calcined nano-size grains.

2. Experimental

2.1 *Synthesis*

Al_2O_3–13 wt% TiO_2 composite powder was synthesized by using reagent grade aluminium nitrate [Al $(NO_3)_3$], titanium dioxide [TiO_2 (99.0%)], nitric acid (HNO_3), sulphuric acid (H_2SO_4) and ammonia solution (NH_3) as the preliminary materials. Ti-nitrate solution was prepared using the commercially available TiO_2. Details of the preparation of Ti-nitrate solution are described elsewhere [14]. In polymer-assisted co-precipitation technique, initially calculated amount of titanium nitrate solution is added to 0.5 mol. $Al(NO_3)_3$ solution as required for 13 wt% TiO_2. While heating and stirring, calculated amount of polymer P123-$(C_3H_6O{\cdot}C_2H_4O)_x$ is added in the prepared $Al(NO_3)_3$ solution. This process is continued till the complete dissolution of the polymer takes place and a homogenous solution is achieved. P123, which is known as poly (ethylene glycol)—block—poly (propylene glycol)—block—poly (ethylene glycol) is highly viscous and has molecular weight as 5800. Concentration of polymer is taken as 15, 30 and 100 wt% of the total calculated weight of desired powder. Stirring of the whole solution is done simultaneously to make it completely homogenous. This metal nitrate solution is precipitated very slowly using diluted ammonia solution till the pH value of the complete solution reaches between 9 and 10. Precipitate is centrifuged to remove ammonia till the pH reaches the range of 6–7. Remaining precipitate is washed using ethanol and dried in a hot air oven at a temperature of 60–70°C for 24 h. After drying, it is ground and treated at 600°C for 6 h. Ground powder is calcined at 1000 and 1200°C for 4 h. Pellets of final calcined (1200°C for 4 h) powder were formed by pressing it on a hydraulic press at a load of 4 tons. Sintering of the formed pellets is done using

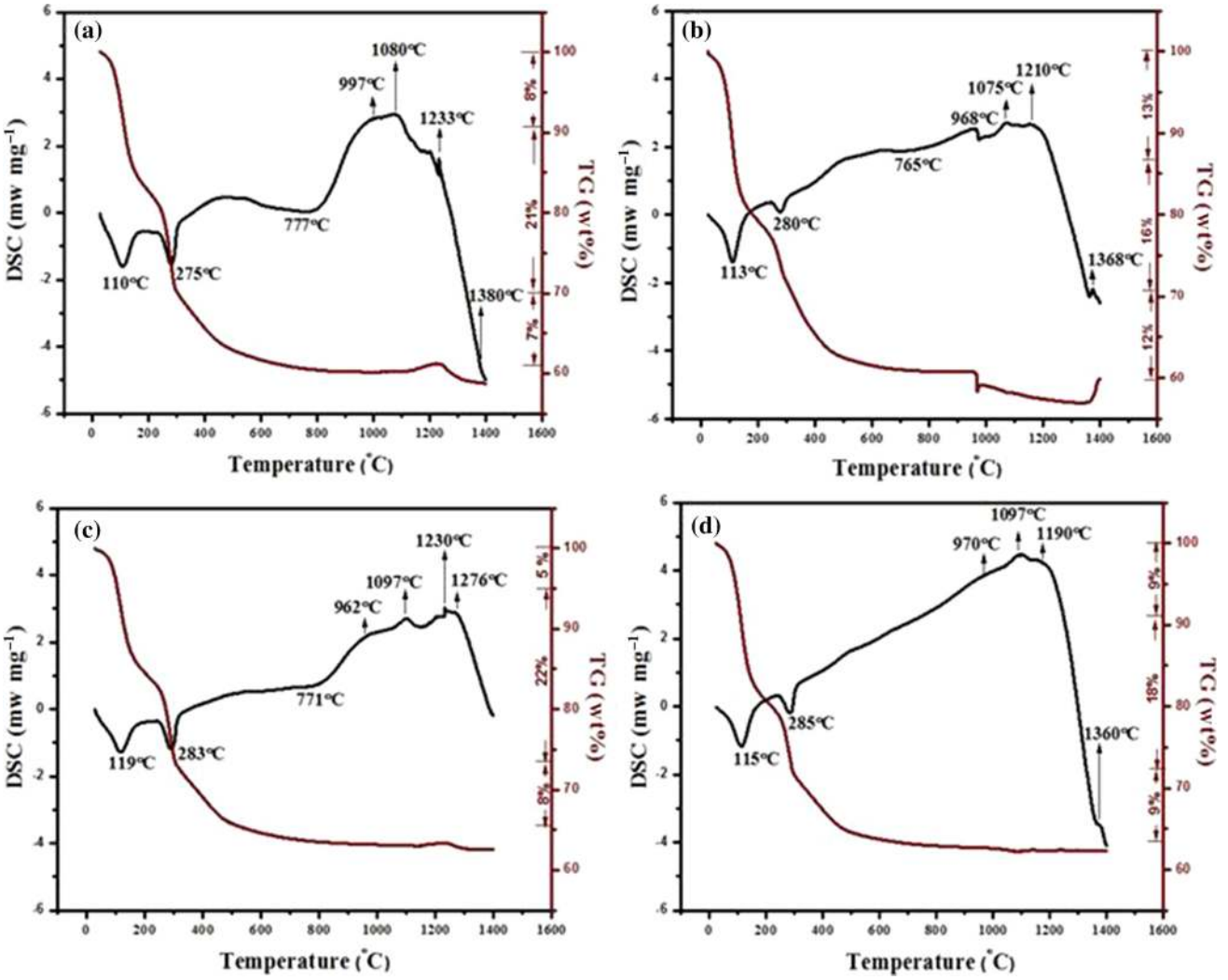

Figure 1. DSC/TGA plot of un-calcined powders (**a**) WOP, (**b**) 15P, (**c**) 30P and (**d**) 100P.

air and atmosphere controlled furnaces at a temperature of 1650°C for 4 h. A nomenclature, e.g., WOP, 15P, 30P and 100P is given for the samples prepared by co-precipitation according to the polymer concentration used during the preparation. Here, P denotes polymer as WOP represents sample prepared without using polymer. 15P, 30P and 100P represent 15, 30 and 100 wt% polymer of the total calculated oxide, respectively, which are used during co-precipitation.

2.2 *Characterization*

Simultaneous differential scanning calorimetry/thermo gravimetric analysis (DSC/TGA) of the dried powder was recorded using STA449C/4/MFC/G (Netzsch, Germany) up to a temperature of 1400°C in argon atmosphere at a rate of 10°C min^{-1}. FTIR spectra of dried un-calcined specimen were recorded using Perkin Elmer, RX-I FTIR spectrometer in the wavelength range of 400–4000 cm^{-1}. Phase determination of the calcined and sintered specimens was studied using Rigaku Desktop Miniflex II X-ray diffractometer employing CuKα radiation and Ni-filter. Diffraction angle was kept from 15 to 80°C and accelerating voltage of 30 kV. Thermal shrinkage behaviour of the green compact was recorded with the help of Netzsch, Germany, DIL 402C dilatometer up to a temperature of 1350°C in an argon atmosphere. Microstructure of the calcined powder and sintered specimen was carried out using FEINOVANANO SEM 450 field emission scanning electron microscope (FESEM). IMAGE-J software was used for the grain size calculation of calcined and sintered specimens. Density measurement was done with the help of Archimedes principle.

3. Results and discussion

3.1 *Study of calcined powders*

3.1a *DSC–TGA*: Figure 1 shows the DSC/TGA curve for powder samples (a) WOP (b) 15P (c) 30P and (d) 100P

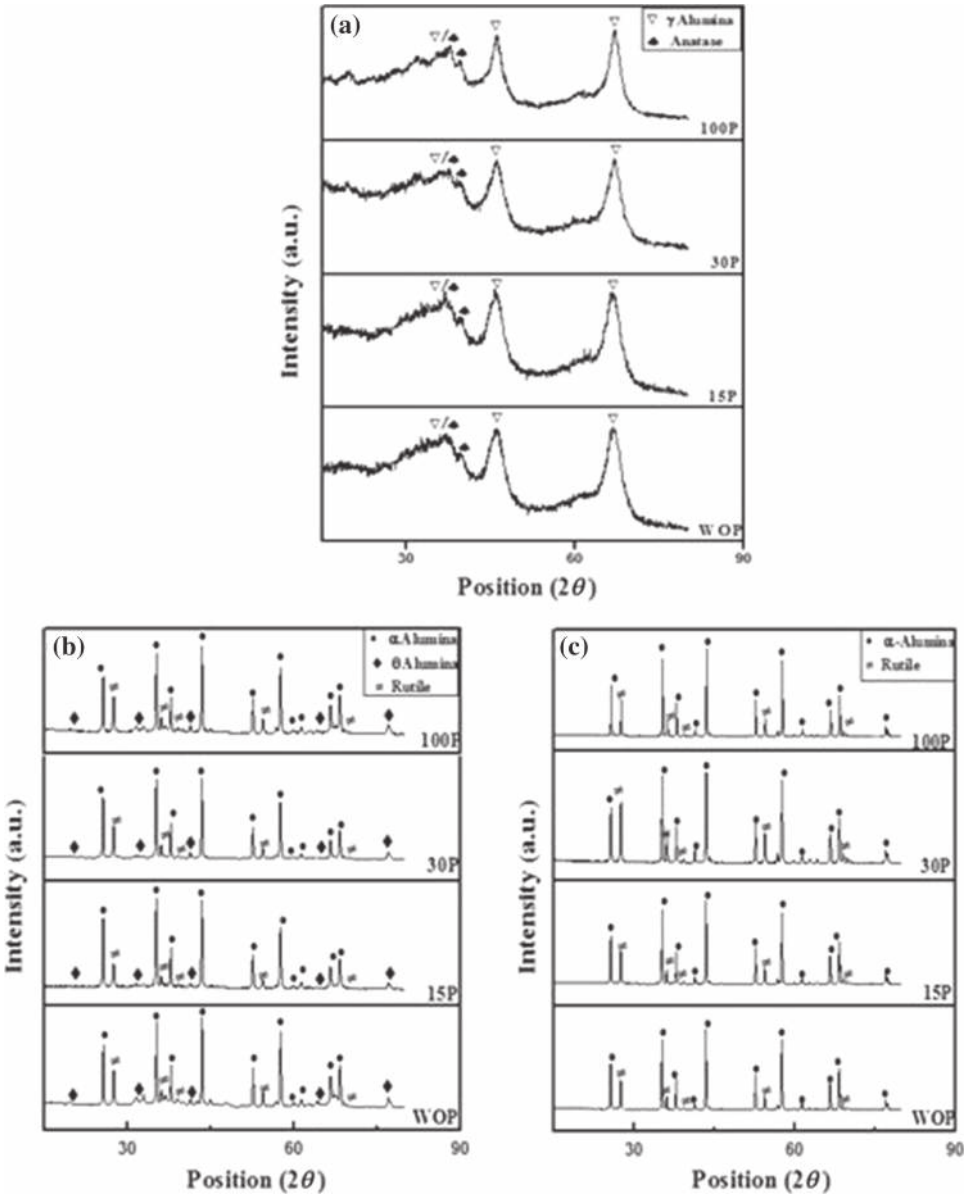

Figure 2. XRD pattern of powders WOP, 15P, 30P and 100P calcined at (**a**) 600°C/6 h, (**b**) 1000°C/4 h and (**c**) 1200°C/4 h.

prepared by the co-precipitation route. First endothermic peak has been observed in the temperature range 110–120°C for all samples, which correspond to the removal of absorbed water. A second endothermic peak is observed at a range 275–285°C, which is related to an early decomposition of gibbsite into γ-alumina phase [15]. At around 700–800°C, a very small change in the DSC curve can be seen, which may be because of the transformation of anatase into rutile phase [16]. Close to 1000°C, an exothermic peak can be distinguished, which may be due to the crystallization and phase transformation of γ-alumina into θ-alumina. Partial transformation from θ to α-alumina has occurred at around 1100°C resulting in another exothermic peak [17]. Complete conversion from θ to α-alumina phase is observed nearly at 1200°C.

The phase transformation behaviour of alumina with temperature has already been investigated which is as follows.

γ-Alumina $\xrightarrow{900-1000^\circ C}$ α-alumina (via combustion synthesis) [18].

γ-AlOOH $\xrightarrow{400^\circ C}$ γ-alumina $\xrightarrow{800^\circ C}$ δ-alumina $\xrightarrow{1000^\circ C}$ θ-alumina $\xrightarrow{1200^\circ C}$ α-alumina (via sol−gel route) [19].

Total weight loss for each powder is observed in a range of 35–39%, which is associated with the water absorption and different phase transformations as mentioned above. It has to be noted that beyond 600°C, a small weight loss is observed. A slight hump near the temperature range of 1275–1380°C is also observed for all samples, which may be responsible for the formation of Al_2TiO_5 phase. Formation of Al_2TiO_5 starts above 1250°C [20], which is attributed to high diffusion rate between the fine alumina and TiO_2 particles. It can be concluded from the DSC/TGA analysis, that the polymer content has a minor influence on DSC/TGA behaviour and formation temperature of Al_2TiO_5 phase in the nanocomposite.

3.1b *X-ray diffraction*: X-ray diffraction patterns of powders (WOP, 15P, 30P and 100P) calcined at temperatures 600°C/6 h, 1000°C/4 h and 1200°C/4 h is shown in figure 2. Powder calcined at 600°C/6 h shows broad peaks, which are associated with γ-alumina phase. Transformation of anatase into rutile phase occurs in a temperature range of 500–800°C, which is reported in the previous literatures [21]. In the present study, no sharp peaks of TiO_2 were observed for the powder calcined at 600°C. Only a few minor peaks of anatase with very low intensity were observed, which means that only anatase phase is present up to this temperature and rutile is absent. The conversion from anatase to rutile is expected to occur between 700 and 800°C. The slight change in DSC plot in this range of temperature can be correlated to the phase transformation from anatase to rutile. Powder calcined at 1000°C/4 h shows sharper peaks with increased crystallinity and the presence of both α-alumina and rutile as major phases [22]. The presence of θ-alumina in a small amount can also be seen up to this temperature. These phase changes can also be confirmed with DSC/TGA analysis as an exothermic peak near 1000°C. The powder, calcined at 1200°C/4 h, shows well crystalline peaks of α-alumina and rutile phases. No Al_2TiO_5 phase is formed till 1200°C. Therefore, it is concluded that up to a temperature of 1000°C, γ-alumina has been converted into α-alumina and some has been remained as θ-alumina. However, at 1200°C, complete conversion into α-alumina has been observed. A slight increase in intensity can be seen in sample 30P as compared to other three samples. XRD results are in the confirmation with the DSC/TGA results for phase formation at different temperature.

3.1c *Dilatometric analysis*: Figure 3 shows the shrinkage behaviour of compacted rectangular bar-shaped specimens of calcined (600°C/6 h) powders of (a) WOP (b) 15P (c) 30P (d)100P. Three step shrinkage behaviours can be seen in the dilatometric curve for each specimen. First step has been observed at around 900–1000°C, which is due to the phase formation of rutile followed by transformation of γ-alumina into θ and α-alumina. The second step change is around 1100–1200°C, which is attributed to the complete conversion into α-alumina. These changes at different temperatures can also be confirmed from the XRD and DTA–TGA plots. Next step

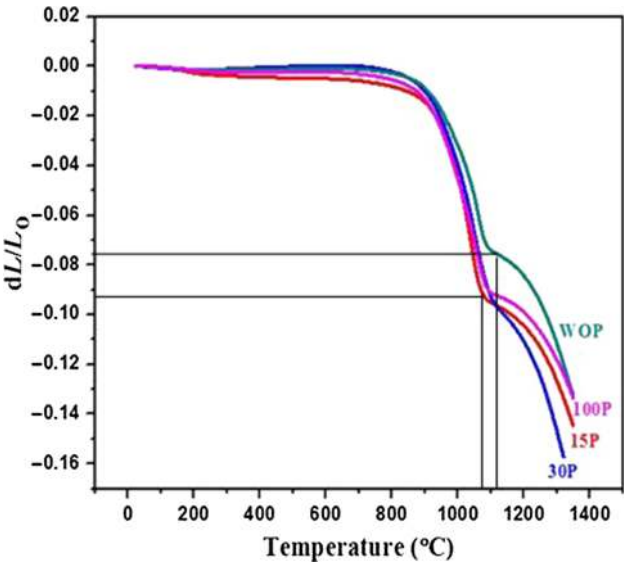

Figure 3. Shrinkage behaviour of compacted rectangular bar-shaped specimens of calcined (600°C/6 h) powders of (**a**) WOP, (**b**) 15P, (**c**) 30P and (**d**)100P.

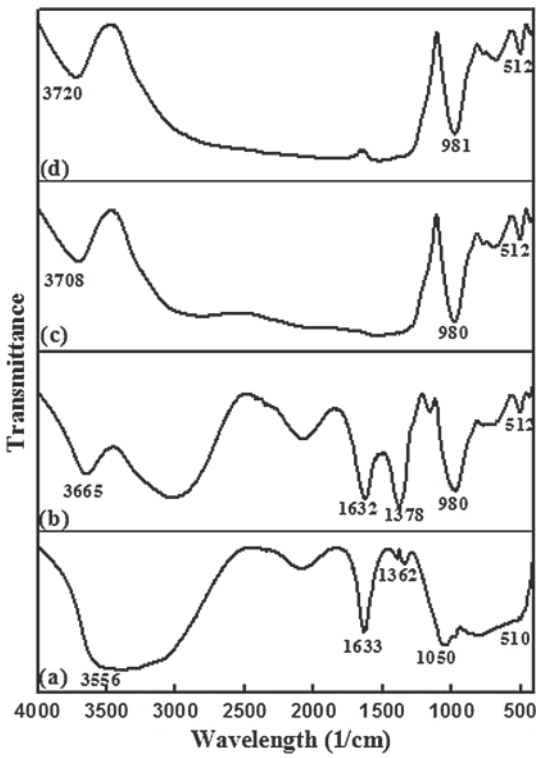

Figure 4. FTIR of un-calcined samples: (**a**) WOP, (**b**) 15P, (**c**) 30P and (**d**) 100P.

shrinkage can be seen above 1300°C, which may be due to the formation of Al_2TiO_5 phase. With increasing polymer content, shrinkage curves have been shifted to lower temperature values, which are due to fine particle size and high reactive nature of the powder. Jayasankar *et al* [23] reported the

onset of shrinkage at around 1100°C for Al_2O_3–20 wt% TiO_2 composites prepared by sol–gel route. The next shrinkage was reported around 1250–1320°C due to the Al_2TiO_5 phase formation.

3.1d *FTIR spectra*: Figure 4 shows the FTIR spectra of uncalcined powder samples (a) WOP (b) 15P (c) 30P (d) 100P in the wavenumber range of 400–4500 cm^{-1}. All four samples show broad band in a range of 3400–3700 cm^{-1}, which corresponds to the adsorbed surface water molecules and O–H vibrations of the group Al–OH and Ti–OH. Again, for the samples WOP and 15P, a narrow peak near 1632 cm^{-1} is seen, which can be again attributed to surface adsorbed water and OH bending modes. The presence of Al=O stretching vibrations can be seen in a range of 1362–1378 [24]. The band near 510 and 980 cm^{-1} are assigned to Ti–O bond vibrations and Al–OH connection for octahedrally co-ordinated Al, respectively [25]. Previous studies have reported the FTIR of pure polymer Pluronic P123 [26–28]. The characteristic bands of CH_3, CH_2, and CH in P123 are located at 2,980, 2,922 and 2,851 cm^{-1}, which are absent in our samples. In the present study, there are no bands attributing to the presence of Pluronic P123 in the FTIR of dried powder samples. Therefore, it is expected that the polymer has been removed during centrifuge washing.

3.1e *Microstructure*: Figure 5 shows FESEM micrograph of powder sample WOP after calcination at 1200°C/4 h. SEM images were captured at different magnifications (a) 10,000× (b) 50,000× and (c) 60,000×. Homogenous distributions and well-defined boundaries can be observed from the micrograph of sample WOP. Observed particle size for sample WOP was found in the range of 0.786–2.12 μm. Figure 6 shows FESEM micrograph (100,000×) for powder samples (a) 15P (b) 30P (c) 100P calcined at a temperature (1200°C/4 h). Particle size of the samples was obtained in the range of 61–173, 41–138 and 29–75 nm for samples 15P, 30P and 100P, respectively. It is clearly observed from the FESEM micrograph (figures 5 and 6) that the particle size of sample without polymer content is in the range of microns, whereas it has been reduced with increasing polymer content during synthesis. Morphology of the powder particles has also improved with increasing polymer content along with the presence of a well-defined boundary of the rounded grains formed in samples, 15P and 30P. For sample 100P, further reduction in particle size can

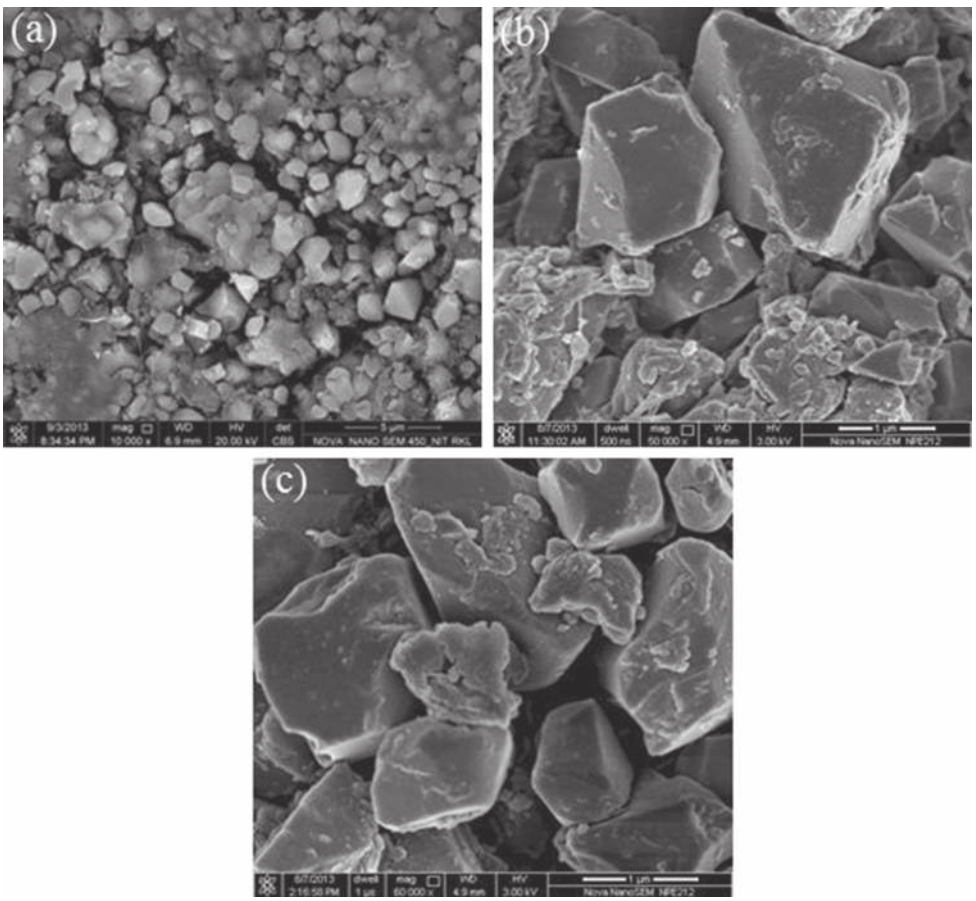

Figure 5. FESEM micrograph of WOP powder (calcined at 1200°C/4 h) at magnification (**a**) ×10,000, (**b**) ×50,000 and (**c**) ×60,000.

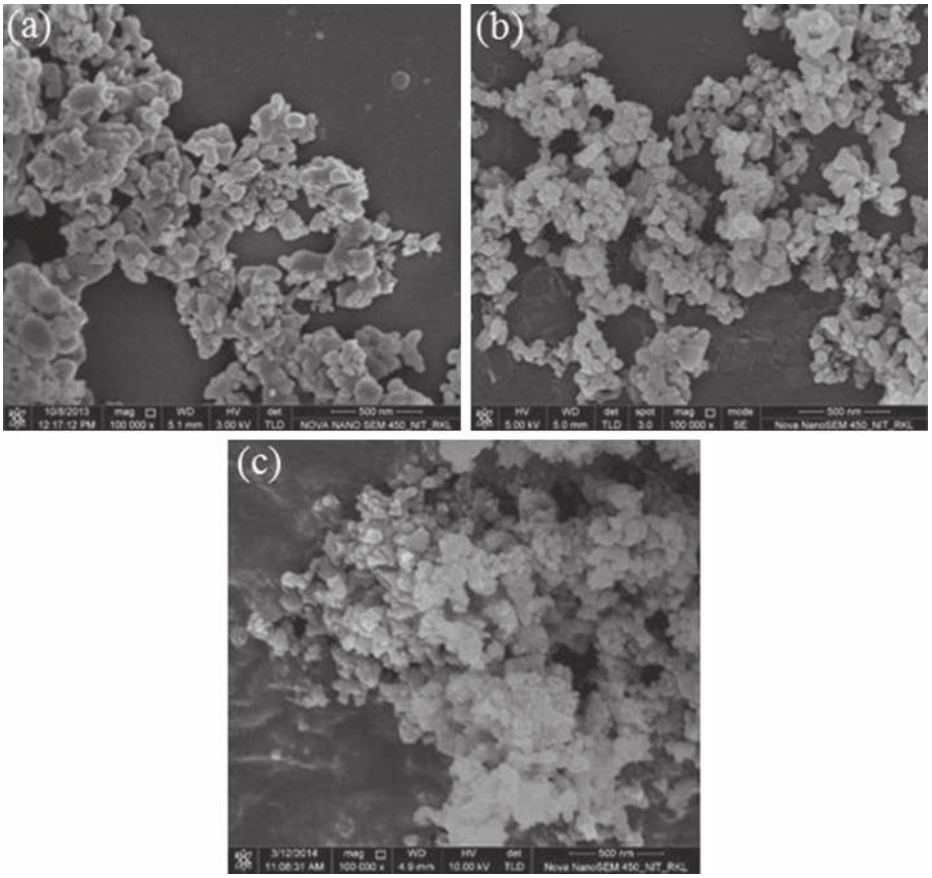

Figure 6. FESEM micrograph (100,000×) of calcined powders at 1200°C/4 h for (**a**) 15P, (**b**) 30P and (**c**) 100P.

be clearly observed but aggregation of particles in the final calcined powders can also be seen in the micrograph.

3.2 *Study of sintering behaviour*

3.2a *X-ray diffraction*: Figure 7 shows the XRD pattern for the samples WOP, 15P, 30P and 100P sintered at 1650°C/4 h. The presence of Al_2TiO_5 (AT) phase along with α-Al_2O_3 has been observed in each sample. A very small amount of TiO_2 has also been observed. It means that TiO_2 is reacting with Al_2O_3 and forming an AT phase, which is stable at room temperature. It is also to be mentioned that the peak intensity has been increased with increasing polymer content, which confirms the enhancement of Al_2TiO_5 phase. The maximum peak intensity is observed for sample 30P sintered at 1650°C/4 h. AT phase formation starts around 1300°C, which has already been confirmed from the DSC/TGA data, dilatometric data and above-mentioned references.

3.2b *Density measurement*: Table 1 shows the density of specimen (a) WOP (b) 15P (c) 30P (d) 100P sintered at 1650°C/4 h. It can be observed from the table that density has improved with increasing polymer concentration during synthesis. Sample WOP is found to have the relative density of 92%. Density has improved for sample 15P, which is around 94%. Maximum relative density of around 96% is achieved for sample 30P. It is to be noted that better density has been achieved for samples prepared by polymer-assisted co-precipitation route. Again a decrease in relative density has been observed for specimen 100P (around 93%). This reduced density may occur because of the nanopowder aggregation of sample 100P during calcination, which may result in cracks when sintering takes place. This may have attributed to the reduction in density.

3.2c *Microstructure*: Figure 8 shows the FESEM micrograph of specimen (a) 15P and (b) 30P sintered at a temperature of 1650°C/4 h at a magnification of 5000×. It shows that a highly dense structure is achieved by the polymer-assisted co-precipitation route. Regular shape and well-defined distribution of grains is also evident from the micrograph. Final phase formation is attributed to the diffusion between synthesized nano size particles. As shown in figure 8, micro

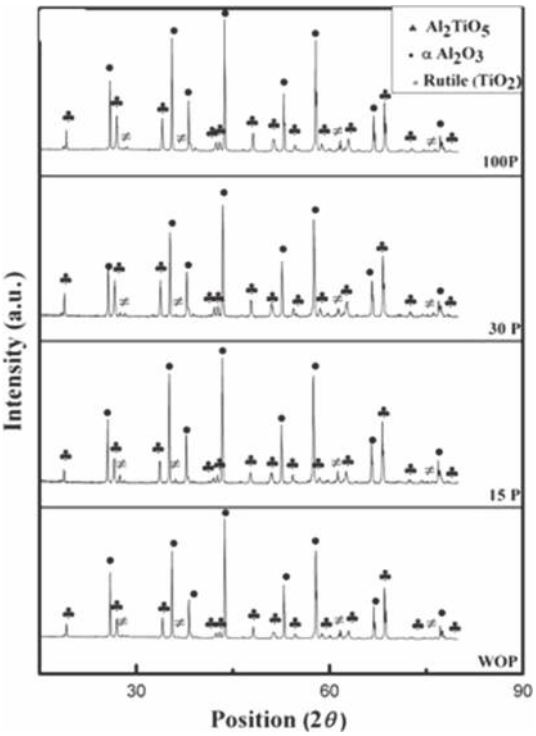

Figure 7. XRD pattern of pellets sintered at 1650°C.

Table 1. Density of sintered samples.

Sample	Sintering temperature	Calculated density	Relative density (%)
WOP	1650°C/4 h	3.65	92
15P	1650°C/4 h	3.72	94
30P	1650°C/4 h	3.80	96
100P	1650°C/4 h	3.70	93

cracks (marked on the figure itself) are formed in samples sintered at 1650°C/4 h, which may be due to the anisotropy in thermal expansion of Al_2TiO_5. This anisotropic nature of the material is attributed to the resistance against thermal shock [29].

4. Conclusion

An Al_2O_3–TiO_2 composite powder containing 13 wt% TiO_2 has been prepared by polymer-assisted co-precipitation technique by varying the concentration of polymer Pluronic P123. FTIR results illustrate the removal of polymer content during washing. From XRD and DSC/TGA analysis, α-alumina and rutile phases were observed in powder calcined at 1200°C/4 h, but the phase formation of Al_2TiO_5 is not visible up to this temperature. Addition of polymer content during precipitation significantly reduces the particle size. With the addition of polymer content, particle size of calcined powders decreases in the range of 29–75 nm. However, the addition of a very high polymer concentration (i.e., 100 wt%) resulted in agglomeration between particles. In the present investigation, 30P has been found to show improved results. Samples prepared by polymer-assisted co-precipitation route have better sinterability, as the onset temperature for polymer containing samples is found to be reduced due to their nanosize. Al_2O_3–TiO_2 nanocomposite powder can be sintered at 1650°C with more than 96% of relative density. Phase analysis of sintered sample shows formation of Al_2TiO_5 phase. With increase in polymer content, peak intensity of Al_2TiO_5 phase is also enhanced. It is found to be at a maximum concentration of 30 wt%. FESEM analysis of sintered pellet shows a well-defined dense structure. Formation of the Al_2TiO_5 phase is attributed to the diffusion between fine alumina and TiO_2 particles.

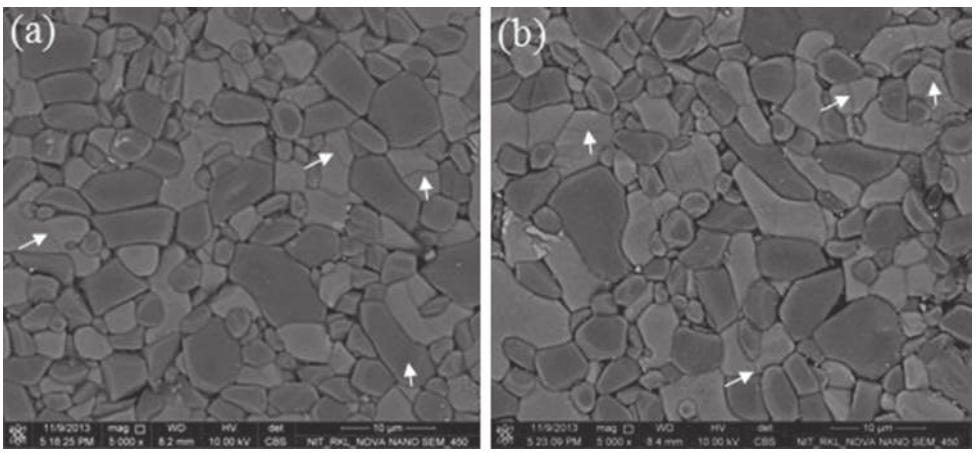

Figure 8. FESEM micrograph of pellets sintered at 1650°C: (**a**) 15P and (**b**) 30P.

References

[1] Niihara K and Nakahira A 1991 *Ceram. Soc. Jpn.* **404** 479
[2] Wang Y M, Tian H, Shen X E, Wen L, Ouyang J H, Zhou Y *et al* 2013 *Ceram. Inter.* **39** 2869
[3] Vlasova M, Kakazey M, Coeto B S, Aguilar P A M, Rosales I, Martinez A E *et al* 2012 *Sci. Sint.* **44** 17
[4] Goberman D, Sohn Y H, Shaw L, Jordan E and Gell M 2002 *Acta Mater.* **50** 1141
[5] Shaw L, Goberman D, Ren R, Gell M, Jiang S, Wang Y *et al* 2000 *Surf. Coat. Technol.* **130** 1
[6] Okamura H, Barringer E A and Bowen H K 1986 *J. Am. Ceram. Soc.* **69** C-22
[7] Jayasankar M, Ananthakumar S, Mukundan P, Wunderlich W and Warrier K G K 2008 *J. Solid State Chem.* **181** 2748
[8] Landeros J O, Yáñez C G, Juárez R L, Velasco I D and Pfeiffer H 2012 *J. Adv. Cer.* **1** 204
[9] Huang Y T, Imura M and Nemoto Y 2011 *Sci. Tech. Adv. Mater.* **12** 1
[10] Mosayebi Z, Rezaei M, Hadian N, Kordshuli F Z and Meshkani F 2012 *Mater. Res. Bull.* **47** 2154
[11] Segadaes A M, Morelli M R and Kiminami R G A 1998 *J. Eur. Ceram. Soc.* **18** 771
[12] Ibrahim D M, Mostafa A A and Khalil T 1999 *Ceram. Int.* **25** 697.
[13] Arenas I B and Gil O 2003 *J. Mater. Process. Tech.* **838** 143
[14] Mazumder R and Sen A 2008 *J. Eur. Ceram. Soc.* **28** 2731
[15] Hernandez T and Bautista M C 2005 *J. Eur. Ceram. Soc.* **25** 663
[16] Abd El-Rady A, Abd El-Sadek M, El-Sayed B M and Assaf F H 2013 *Adv. Nanopart.* **2** 372
[17] Chen D and Jordan E H 2009 *J. Sol-Gel Sci. Tech.* **50** 44
[18] Sathyaseelan B, Baskaran I and Sivakumar K 2013 *Soft Nanosci. Lett.* **3** 69
[19] Sarkar D, Adak S and Mitra N K 2007 *Compos. Part A: Appl. Sci. Manuf.* **38** 124
[20] Jayasankar M, Hima K P, Ananthakumar S, Mukundan P, Pillai P K and Warrier K G K 2010 *Mater. Chem. Phys.* **124** 92
[21] Ahmed M A and Abdel Messih M F 2011 *J. Alloys Compd.* **509** 2154
[22] Gupta P, Kumar D, Parkash O and Jha A K 2013 *Bull. Mater. Sci.* **36** 859
[23] Jayasankar M, Ananthakumar S, Mukundan P and Warrier K G K 2007 *Mater. Lett.* **61** 790
[24] Vasconcelos D C L, Nunes E H M and Vasconcelos W L 2012 *J. Non-Cryst. Solids* **358** 1374
[25] Adamczyk A and Długon E 2012 *Spectrochim. Acta Part A* **89** 11
[26] Julián-López B, Boissière C, Chanéac C, Grosso D, Vasseur S, Miraux S *et al* 2007 *J. Mater. Chem.* **17** 1563
[27] Cao S W, Zhu Y J, Wu J, Wang K W and Tang Q L 2010 *Nanoscale Res. Lett.* **5** 781
[28] Rezaei M, Khajenoori M and Nematollahi B 2011 *Powder Technol.* **205** 112
[29] Hasselman D P H 1969 *J. Eur. Am. Soc.* **52** 600